Title

Omega-3 fatty acids reduce obesity-induced tumor progression independent of GPR120 in a mouse model of postmenopausal breast cancer

Journal

Oncogene, 34(27)

ISSN

0950-9232

Authors

Chung, H

Lee, YS

Mayoral, R

et al.

Publication Date

2015-07-01

DOI

10.1038/onc.2014.283

Peer reviewed

Omega-3 fatty acids reduce obesity-induced tumor progression independent of GPR120 in a mouse model of postmenopausal breast cancer

Heekyung Chung[1], Yun Sok Lee[1], Rafael Mayoral[1,2], Da Young Oh[1], Justin T Siu[3], Nicholas J. Webster[1,4,5], Dorothy D. Sears[1,4], Jerrold M. Olefsky[1,4], Lesley G. Ellies[3,4*]

Running title: Omega-3 fatty acids reduce obesity-induced mammary tumor growth

[1] Department of Medicine, Division of Endocrinology and Metabolism
University of California, La Jolla, CA 92093, USA
[2] Biomedical Network Center for the study of Hepatic and Digestive Diseases (CIBERehd), Madrid, Spain
[3] Department of Pathology
University of California, La Jolla, CA 92093, USA
[4]Moores Cancer Center
University of California, La Jolla, CA 92093, USA
[5]San Diego VA Healthcare System, San Diego, CA 92161, USA
[*] Correspondence: lellies@ucsd.edu

Address to correspondence to Lesley G. Ellies, Ph.D.

Abstract

Obesity and inflammation are both risk factors for a variety of cancers including breast cancer in postmenopausal women. Intake of omega-3 polyunsaturated fatty acids (ω-3 PUFAs) decreases the risk of breast cancer, and also reduces obesity-associated inflammation and insulin resistance, but whether the two effects are related is currently unknown. We tested this hypothesis in a postmenopausal breast cancer model using ovariectomized (OVX), immune-competent female mice with orthotopically injected with Py230 mammary tumor cells. Obesity, whether triggered genetically or by high-fat diet (HFD) feeding, increased inflammation in the mammary fat pad and promoted mammary tumorigenesis. The presence of tumor cells in the mammary fat pad further enhanced the local inflammatory milieu. TNF-α was the most highly up-regulated cytokine in the obese mammary fat pad, and we observed that TNF-α dose-dependently stimulated Py230 cell growth *in vitro*. An ω-3 PUFA-enriched HFD (referred to as fish oil diet, FOD) reduced inflammation in the obese mammary fat pad in the absence of tumor cells and inhibited Py230 tumor growth *in vivo*. Although some anti-inflammatory effects of ω-3 PUFAs were previously shown to be mediated by the G protein-coupled receptor 120 (GPR120), the FOD reduced Py230 tumor burden in GPR120 deficient mice to a similar degree as observed in WT mice, indicating that effect of FOD to reduce tumor growth does not require GPR120 in the host mouse. Instead, *in vitro* studies demonstrated that ω-3 PUFAs act directly on tumor cells to activate JNK, inhibit proliferation and induce apoptosis. Our results show that obesity promotes mammary tumor progression in this model of postmenopausal breast cancer and that ω-3 PUFAs inhibit mammary tumor progression in obese mice, independent of GPR120.

Keywords: obesity, mammary tumors, inflammation, postmenopausal breast cancer, ω-3 PUFAs, GPR120

Introduction

Practical strategies to reduce the harmful sequelae of the worldwide obesity epidemic are paramount for reducing the future medical burden to society. There is abundant evidence linking obesity to the overall risk for several cancers including endometrial, colorectal, prostate, pancreatic and postmenopausal breast cancer [6, 13, 15, 22, 33]. Furthermore, in breast cancer obesity is associated with a higher incidence of more aggressive triple negative breast tumors and reduced survival, regardless of menopausal status [24]. Why obesity increases cancer risk is not known but it is thought to be related to increased tissue inflammation, insulin resistance, and/or hyperinsulinemia. Thus, dietary intervention is a potential means to mitigate this risk. Altering the balance between dietary omega-3 (ω-3) and ω-6 polyunsaturated fatty acids (PUFAs) has received considerable attention as an approach for disease prevention [5, 29] and several epidemiological and preclinical studies have suggested an anti-tumor effect of ω-3 PUFAs on breast cancer [12, 28, 37]. The complex mechanisms by which ω-3 PUFAs, particularly eicosapentaenoic acid (EPA) and docosahexaenoic acid (DHA), exert their anticancer effects are not well understood although multiple targets regulating cell proliferation, cell survival, inflammation, angiogenesis and metastasis may be involved [10].

We have shown that the G protein-coupled receptor 120 (GPR120) is a functional ω-3 PUFA receptor that mediates potent insulin sensitizing and anti-diabetic effects *in vivo* by repressing macrophage-induced adipose tissue inflammation in obese mice [19]. The state of chronic, low grade inflammation arising in obesity is characterized by infiltration of M1-type adipose tissue macrophages (ATMs), cells that secrete high levels of proinflammatory cytokines, TNF-α, IL1β and IL-6 and are considered to be major contributors to tissue inflammation and insulin resistance in obesity [14, 20]. In breast cancer patients, increased circulating TNF-α levels

are positively correlated with tumor cell proliferation, tumor stage and lymph node metastasis [3, 27]. Since TNF-α signals through the JNK and NFκB pathways and ω-3 PUFAs can inhibit these pathways by sequestering TAB1 in obese mice [19], we tested whether obesity induced inflammation could be ameliorated by ω-3 PUFAs in a postmenopausal breast cancer model.

We have used orthotopic injection of the Py230 breast cancer cell line into syngeneic ovariectomized (OVX), immune-competent mice to demonstrate that obesity, induced either by high-fat diet (HFD) or genetically, increases inflammation in the mammary fat pad and concurrently promotes mammary tumor growth. While ω-3 PUFAs reduced inflammation in the mammary fat pad in the absence of tumor cell injection, they inhibited mammary tumor growth independent of inflammation and GPR120 expression in the mammary fat pad. We demonstrate that DHA inhibits Py230 mammary tumor cell growth directly via induction of apoptosis *in vitro*. Our results suggest that further investigation into the mechanisms by which ω-3 PUFAs can impact breast cancer is warranted.

Results

HFD or genetically-induced obesity promotes mammary tumor growth

We first examined tumor progression in HFD-induced or genetically obese OVX mice to address whether the origin of the obesity plays a role in the promotion of postmenopausal breast cancer. As expected and consistent with previous reports [7, 31], HFD feeding led to body weight gain and increased mammary fat pad weight in both wild type (WT) and ob/+ heterozygous (Het) mice compared to their normal chow (NC)-fed counterparts (Figure 1A and Figure S1). NC-fed ob/ob mice, which are hyperphagic from birth due to a homozygous mutation in the leptin gene, had significantly greater body weights than either WT or Het mice fed HFD, and their body

weights were further increased by HFD-feeding (Figure 1A). We assessed mammary tumor growth in these mouse groups seven weeks after injection of Py230 tumor cells (Figure 1B). HFD significantly increased tumor burden in WT and Het mice compared to NC (51% and 63% respectively). Obese ob/ob mice fed NC showed tumor growth equivalent to that observed in WT and Het mice fed HFD and the HFD feeding did not significantly increase tumor burden in the ob/ob mice (Figure 1B). Regression analysis of tumor weight versus body weight revealed that the mammary tumor burden was positively correlated with body weight across all strains and diets ($r = 0.522$, $p < 0.001$, Figure 1C). These data indicate that obesity, whether induced by HFD feeding or leptin deficiency, significantly increases mammary tumor growth and validate this OVX mouse model for translational postmenopausal breast cancer studies.

Obesity induces inflammation in the mammary fat pad

Inflammation is a potential link between obesity and breast cancer [8, 16, 30]. To interrogate the role of inflammation in mammary tumor growth, we examined macrophage infiltration, macrophage polarization and cytokine gene expression in the mammary fat pad.

Obesity in mice, regardless of its origin, induced significantly greater M1-type, proinflammatory macrophage infiltration in the mammary fat pad compared to lean controls, as determined by flow cytometry assessment of $F4/80^{+}CD11b^{+}CD11c^{+}$ expression (Figure 2A). Data compiled across all the mouse groups indicated a consistent 3-4-fold increase in proinflammatory M1-type macrophages in obese mice compared to lean mice (Figure 2B). This infiltration was highly correlated with mouse body weight ($r = 0.746$, $p < 0.001$, Figure 2C).

The proinflammatory nature of the infiltrating macrophages was confirmed by real time PCR analysis showing significantly higher expression of M1-type macrophage associated proinflammatory genes *Ccl2* (monocyte chemotactic protein, MCP-1) and *Tnf* in obese relative

to lean mice (Figure 2D). No significant difference was observed in the expression of several other M1-type macrophage associated proinflammatory genes, *Il1b* (IL-1β), *Il6* (IL-6), and *Nos2* (iNOS) (Figure S2). Obesity did not result in any significant difference in expression of M2-type macrophage associated anti-inflammatory genes such as *Arg1* (arginase 1, Arg-1) and *Clec10a* (macrophage galactose-type C-type lectin 1, MGL-1) in the mammary fat pad (Figure S3). Expression of the inflammatory mediators keratinocyte-derived chemokine (KC/*Cxcl1*), MCP-1, IL-1β, IL-6 and TNF-α was evaluated in mammary tumor extracts using a cytokine multiplex assay. There was no significant difference between lean and obese mice (Figure S4), demonstrating that obesity increases inflammation in the mammary fat pad but not in mammary tumors in our model. Furthermore, analysis of hematoxylin and eosin (H&E) and F4/80 stained sections of the tumors revealed neither significant morphological changes nor differences in macrophage infiltration between tumors from lean or obese mice (data not shown).

TNF-α enhances tumor cell proliferation and activates NFκB and JNK signaling in Py230 cells

Since we observed significantly increased TNFα and MCP-1 gene expression in the obese mammary fat pad, we examined the effects of TNFα and MCP-1 on Py230 cell growth *in vitro*. TNFα dose-dependently stimulated Py230 cell proliferation from day 6 post-treatment onwards, but MCP-1 had no effect (Figure 3A). The TNF Receptor (TNFR) signals via the NFκB and JNK pathways so we tested the involvement of these pathways in the proliferative response. Inhibition of the JNK pathway with SP600125 reduced the basal proliferation of the Py230 cells and eliminated the enhanced proliferation with TNFα (Figure 3B). In contrast, inhibition of the NFκB pathway with JSH-23 reduced the basal proliferation but had no effect on the TNFα-promoted proliferation (Figure 3B).

Treatment of Py230 cells with TNF-α caused an increase in JNK, TAK1 and IKKα/β phosphorylation and degradation of IκBα, suggesting that JNK and NFκB signaling are activated in response to TNF-α in Py230 cells (Figure 3C). Together, these results suggest that TNF-α production in the mammary fat pad of obese mice may play a direct role in tumor growth by stimulating tumor cell proliferation.

Omega-3 PUFAs ameliorate obesity-induced mammary fat pad inflammation

Omega-3 PUFAs signaling via GPR120 and Toll-like receptor 4 (TLR4) utilize the same NFκB and JNK pathways as TNF−α, so they could potentially interfere with these proliferative signals [19, 34]. Among dietary fat subtypes, ω-3 PUFAs offer the most promise for reducing the risk of carcinogenesis [18, 21]. So we tested whether HFD supplementation with ω-3 PUFAs derived from fish oil (FOD, fish oil diet) could reduce inflammation in the mammary and perigonadal fat pads of obese OVX mice in the absence of tumor formation. Mice were fed normal HFD or an isocaloric HFD containing 24% DHA and 6% EPA (FOD). In perigonadal fat tissue, FOD-fed OVX female mice showed reduced expression of macrophage marker genes (F4/80 and CD11c) and M1-type macrophage proinflammatory mediator genes such as MCP-1 and TNF-α compared to HFD-fed mice (Figure 4A), as we had previously observed in epididymal adipose tissue from male mice [19]. In contrast to our previous findings in epididymal adipose tissue from male mice, IL-6 expression was increased and IL-1β and iNOS expression was not altered in the current studies (Figure 4A). In addition, FOD-fed mice tended to increase expression of Arg-1 but significantly decrease expression of macrophage mannose receptor 1 (MMR/*Mrc1*) compared to HFD-fed mice, showing mixed results for M2-type macrophage anti-inflammatory genes (Figure 4A). Inflammation in the mammary fat pad was also significantly decreased by ω-3 PUFAs. FOD-fed mice showed a significant reduction of F4/80, CD11c,

MCP-1, TNF-α, and MMR gene expression in the mammary fat pad whereas IL-6 and Arg-1 gene expression was significantly increased compared to HFD-fed mice (Figure 4B). These data indicate ω-3 PUFAs can reduce inflammation in both the perigonadal and mammary fat depots of obese OVX mice in the absence of tumor cells.

Omega-3 PUFA inhibits mammary tumor growth

Since our HFD studies suggested that inflammation in the mammary fat pad was driving tumor progression and the FOD reduced mammary fat pad inflammation, we hypothesized that a FOD would reduce Py230 tumor growth. Indeed, FOD-fed mice had a significantly reduced mammary tumor burden (28%) compared to HFD-fed mice of equivalent weight (Figure 5A and Figure S5). As we observed in our initial HFD study (Figure S4), the FOD did not alter gene expression of macrophage markers or inflammatory mediator such as TNF-α, iNOS, MCP-1, IL-1β, IL-6, Arg-1 and MMR in mammary tumors (Figure S6). We observed no difference in GPR120 gene expression in mammary tumors between HFD- and FOD-fed mice (Figure 5B) but GPR120 expression was significantly higher in the mammary fat pad compared to mammary tumors from HFD-fed mice (Figure 5B). Unexpectedly and unlike the mammary fat pads of naïve mice (Figure 4B), the mammary fat pads of tumor-bearing mice did not show significant differences in macrophage marker or inflammatory cytokine gene expression on the FOD compared to the HFD-fed mice (Figure 5C), and, indeed, some markers tended to increase, suggesting that the presence of tumor cells modulates the effect of the FOD in the mammary fat depot. The FOD did have its expected effect to reduce inflammation in perigonadal fat, however, as expression of F4/80, CD11c and TNF-α tended to be lower (Figure 5D). Due to the discrepant results with inflammatory markers between naïve and tumor bearing mice, we performed a direct comparison of these markers in the mammary fat pad and perigonadal fat in uninjected obese

mice or in tumor-cell injected obese mice. In HFD-fed mice, tumor cell injection significantly increased F4/80, CD11c and IL-1β gene expression and decreased TNF-α expression and tended to decrease IL-6 expression in the mammary fat pad (Figure 5E), but did not in perigonadal fat where IL-1β and IL-6 were significantly increased (Figure 5F).

Omega-3 PUFA effects on mammary tumor growth are independent of GPR120

We have shown that a FOD reduces obesity-induced inflammation in adipose tissues from male mice via GPR120-mediated signaling and improves metabolic defects in these mice [19]. Since we showed that the FOD could reduce tumor burden but paradoxically not inflammation in tumor bearing mice, we wondered whether GPR120 mediates the tumor inhibitory effect of FOD as we had previously seen for the anti-inflammatory effect in male mice.

To directly test this hypothesis, we injected GPR120 positive Py230 tumor cells into the mammary fat pad of GPR120 knock out (KO) mice. The KO mice, fed FOD for nine weeks prior to tumor cell injection, showed significantly reduced mammary tumor burden (38%) compared to HFD-fed KO mice (Figure 5G), demonstrating that contrary to our hypothesis, GPR120 expression in the mammary fat pad was not essential for the inhibitory effect of the FOD on mammary tumor growth.

Omega-3 PUFAs inhibit Py230 mammary tumor cell growth via induction of apoptosis *in vitro*

Since the FOD did not alter inflammation in the mammary tumors themselves (Figure S4) we tested whether a FOD could inhibit mammary tumor progression by decreasing cell proliferation and/or increasing apoptosis in tumors. Ki-67 and TUNEL immunohistochemical staining of mammary tumors revealed a high degree of variability in cell proliferation and

apoptosis between tumors and no significant differences were observed between mice fed with a HFD or FOD (data not shown).

Relatively small changes in cell growth or apoptosis occurring *in vivo* over time are difficult to measure, so we examined whether ω-3 PUFAs, specifically DHA, could act directly on Py230 tumor cells to reduce mammary tumor cell growth *in vitro*. DHA significantly inhibited Py230 cell growth in a dose-dependent manner (Figure 6A). This DHA-induced cell growth inhibition was also observed in GPR120 KO cells derived from tumors of double transgenic PyVmT/GPR120 KO mice (Figure 6A), indicating that DHA inhibits Py230 tumor cell growth independent of GPR120 signaling in agreement with our *in vivo* tumor growth studies (Figure 5G). In addition, DHA pre-treatment inhibited TNF-α-induced Py230 cell growth (Figure 6B) and blocked NF-κB activation and nuclear translocation stimulated by either TNF-α or LPS in Py230 cells (Figure 6C and Figure S7). Interestingly, DHA treatment itself induced robust JNK phosphorylation, which was maintained after subsequent TNF-α or LPS treatment (Figure 6C). DHA also increased the activities of caspases 3 and 7 and induced apoptosis in Py230 cells (Figure 6D and 6E). Our results suggest that ω-3 PUFAs may suppress mammary tumor growth by directly inhibiting the growth of mammary tumor cells via induction of apoptosis. As activated JNK signaling suppresses insulin signaling in the context of inflammation [19, 26], we tested whether DHA-induced JNK activation in Py230 cells inhibits insulin signaling through AKT. Py230 cells showed high basal AKT phosphorylation, which was not increased by insulin stimulation. DHA treatment significantly increased JNK phosphorylation as we had observed earlier and inhibited both basal and insulin-stimulated AKT phosphorylation (Figure 6F).

Discussion

We have shown that obesity in OVX mice, whether driven by HFD or leptin deficiency, increased macrophage infiltration and inflammation in mammary fat pads and increased growth of orthotopically injected Py230 tumor cells in concordance with other studies examining obesity, inflammation and cancer [23, 31, 32]. We observed that ω-3 PUFA supplementation reduced obesity-associated adipose tissue inflammation in tumor naïve mice but not in tumor bearing mice. Omega-3 PUFA supplementation reduced mammary tumor growth in obese mice and this effect was independent of inflammation or the expression of GPR120 in the host mammary fat pad. TNF-α expression was highly increased in the obese OVX mouse mammary fat pad and we showed that TNF-α stimulates Py230 cell proliferation *in vitro* in a pathway requiring JNK activation. Treatment of Py230 cells with ω-3 PUFA DHA strongly activates JNK, triggering apoptosis and inhibiting the ability of TNF-α to stimulate proliferation. Together, our studies show that TNF-α stimulates Py230 tumor cell proliferation by a mechanism where JNK activation is necessary but not sufficient and where the non-JNK signaling components of TNF-α–induced tumor cell proliferation are blocked by DHA. Such non-JNK targets are interesting for future study. We also made the interesting observation that the presence of tumor cells increases the macrophage content and modulates the inflammatory environment of the mammary fat pad but eliminates the anti-inflammatory effects of ω-3 PUFA.

Numerous studies have demonstrated beneficial, inflammatory disease-modulating effects of ω-3 PUFAs, especially EPA and DHA, that result from decreased inflammatory cytokines and lipid mediators such as prostaglandins, leukotrienes, resolvins and protectins [2, 4]. Epidemiological studies have found that increased ω-3 PUFAs intake is associated with reduced breast cancer risk in humans, particularly in postmenopausal women [9, 22, 25] suggesting a common

link between breast cancer and inflammation-related disease risk. However, the majority of mechanistic animal and cell culture model studies of breast cancer show that the protective effect of ω-3 PUFAs is mediated via suppression of cell proliferation or angiogenesis, or an increase in apoptosis [11, 17, 28, 36].

Some of the anti-inflammatory effects of ω-3 PUFAs are mediated by GPR120 and, indeed, we have previously shown that all anti-inflammatory effects are lost in obese male GPR120 KO mice [12]. Not all actions of GPR120 are beneficial, however. A recent study showed that GPR120 expression was significantly induced in human colorectal tissues and cell lines and activation of GPR120 in colorectal cells promoted angiogenesis and tumor growth *in vivo*, suggesting that GPR120 can function as a tumor promoting receptor in colorectal cancer [35]. We observed that GPR120 expression is much lower in tumors compared to the surrounding mammary fat pad in our breast cancer model, so this discrepancy could be due to specific cancer types (colorectal vs breast) or different species (human and mice). Our studies indicate that GPR120 functions neither to inhibit mammary tumor progression by modulating stromal, mammary adipose tissue inflammation, nor to directly inhibit tumor cell proliferation. Additional studies are necessary to elucidate whether GPR120 plays any role in the development and progression of breast cancer.

Since we observed ω-3 PUFAs inhibit mammary tumor growth and Py230 tumor cell growth *in vitro* independent of GPR120 signaling, we speculate that this ω-3 PUFA effect may be mediated through TLR4, peroxisome proliferator-activated receptors (PPARs), or other G protein coupled receptors (GPRs) and this will be studied in the future. Additional studies are necessary to investigate the underlying signaling pathways involved in DHA induced JNK signaling activation and test whether JNK activation by DHA is required for DHA's mammary

tumor inhibitory properties. In summary, our results suggest that ω-3 PUFAs may suppress mammary tumor growth by directly inhibiting the growth of mammary tumor cells via induction of apoptotic pathways. Further study is needed to clarify the mechanism of action of ω-3 PUFAs and identify new therapeutic targets for obese postmenopausal women with breast cancer.

Materials and Methods

Chemicals and reagents DHA was obtained from Cayman Chemical (Ann Harbor, MI). F12K nutrient medium was obtained from Mediatech, Inc (Manassas, VA) and fetal calf serum (FCS), gentamycin, fungizone from Invitrogen (Carlsbad, CA) and MITO Plus serum extender were obtained from BD Bioscience (San Jose, CA). SP600-125 (JNK inhibitor), JSH-23 (NFκB inhibitor) and LPS were obtained from Sigma Chemical (St. Louis, MO). Recombinant mouse TNF-α and MCP-1were obtained from BioLegend (San Diego, CA).

Animals and Animal Care WT, heterozygous (+/ob, Het) and ob/ob female C57BL/6J mice were purchased and OVX at 6 weeks of age in the Jackson Laboratory (Bar Harbor, ME). WT C57BL/6J and littermate GPR120 KO mice were OVX at 7-8 weeks of age. Mice were fed either NC [12% kcal from fat; Purina 5001, LabDiet (St. Louis, MO)], HFD [60% kcal from fat; D12492, Research Diets (New Brunswick, NJ)] or an isocaloric HFD containing 30% ω-3 PUFAs replacement (FOD; wt/wt; 24% DHA, 6% EPA, Research Diets). Animals were maintained on a 12-h/12-h light/dark cycle with free access to food and water. All animal procedures were in accordance with University of California San Diego research guidelines for the care and use of laboratory animals.

Syngeneic orthotopic tumor model Py230 tumor cells derived from a PyVmT/C57BL6 mouse were used for orthotopic inoculation into the mammary fat pad of mice [1]. One hundred thousand

cells re-suspended in 2 mg/ml matrigel/PBS (Invitrogen, Carlsbad, CA) solution were injected into the right and left thoracic and inguinal mammary fat pads using a 30 gauge needle. To monitor tumor growth in the mammary fat pad, Py230 tumor cell injected mammary glands were examined by finger palpation. Mammary tumor growth was determined by tumor weights. The mammary fat pads, tumors and perigonadal fat were excised, weighed and snap frozen in liquid nitrogen for further studies. Portions of tumors were fixed in 10% buffered formalin for histological analysis. Portions of fat pads were placed in ice cold PBS for the isolation of the stromal vascular cell (SVC) fraction and FACS analysis.

SVC isolation and FACS analysis Mammary fat pads were weighed, rinsed in PBS, and minced in FACS buffer (1% low endotoxin bovine serum albumin in PBS). SVCs were prepared from collagenase (Sigma) digested fat pads and FACS analysis of SVCs for macrophage content and subtypes were performed as previously described [14]. Briefly, SVCs were incubated with Fc block (e-Bioscience, San Diego, CA) for 20 min on ice before staining with fluorescently labeled primary antibodies for 30 min on ice. APC-F4/80 FACS antibody (AbD Serotech, Raleigh, NC), FITC-CD11b and PE-CD11c FACS antibodies (BD Biosciences) were used. Cells were gently washed and resuspended in FACS buffer with propidium iodide (Sigma). SVCs were analyzed by a FACSCalibur with CELLQUEST acquisition and analysis software (BD Bioscience). Unstained, single fluorescence stained and fluorescence minus one stained controls were used for setting compensation and gates.

mRNA isolation and qPCR Total RNA was isolated from mammary fat pads, tumors and perigonadal fat using the Trizol reagent (Invitrogen). First-strand cDNA was synthesized using a MMLV-Reverse Transcriptase and random hexamers (Promega, Madison, MI) and amplified using primers listed in **Table S1**. qPCR was performed using an iTaq Universal SYBR Green

Supermix (Bio-Rad, Hercules, CA) on Step One Plus Real time PCR system (Applied Biosystems, Grand Island, NY). Gene expression levels were calculated after normalization to the standard housekeeping genes *RNA polymerase II (RP II)* and *Glyceraldehyde 3 phospate dehydrogenase (GAPDH)* using the $\Delta\Delta C_T$ method and expressed as relative mRNA level compared with internal control.

Cell Culture Py230 cells, a clonal cell line derived from a PyVmT tumor and GPR120 KO cells derived from a PyVmT/GPR120 KO tumor were maintained in F12K nutrient medium supplemented with 5% (v/v) FCS, 50 μg/ml gentamycin, 2.5 μg/ml fungizone and MITO+ serum extender (1:1000) at 37 C under 5% CO_2. The cell viability assay and apoptosis assay with treatment of vehicle or DHA were performed in F12K nutrient medium supplemented with 2% (v/v) FCS, 50 μg/ml gentamycin and 2.5 μg/ml fungizone.

Cell viability assay The MTT [3-(4.5-dimethylthiazol-2-yl)-2,5-diphenylt3etrazodium bromide] assay was used. Py230 cells were seeded in 96-well plates. The 100 mM stock solution of DHA (dissolved in 200-proof ethanol) was diluted in ethanol first and then in the culture medium immediately at the desired final concentrations before adding to each well for 48hr. The cells were washed once in PBS and 100 μl of MTT (0.5 mg/ml) was added to each well at a final concentration of 50 μg/ml for 3 hours. After incubation the MTT was removed, 100 μl of acidic isopropanol (30 μl of 12 M HCl in 10 ml) was added, and the absorbance was read with a Spectromax 190 microplate reader (Molecular Devices, Sunnyvale, CA) at 560 nm.

Western blotting Cells and tissues were washed with cold PBS on ice and treated with RIPA lysis buffer (Millipore, Temecular, CA) containing a cOmplete protease inhibitor cocktail tablet (Roche, Madison, MI) and a PhosSTOP phosphotase inhibitor cocktail tablet (Roche, Madison, MI). The protein amount was determined using the Bio-Rad protein assay (Bio-Rad). After an

equal amount of protein was loaded in each lane, they were separated by 10% (w/v) SDS-PAGE and then transferred to an Immobilon-P PVDF membrane (Millipore). Target proteins were immunodetected using specific primary antibodies and the horseradish peroxidase (HRP)-conjugated anti-rabbit or anti-mouse IgG (Jackson ImmunoResearch Laboratories, West Grove, CA) was used as a secondary antibody. Positive bands were detected using the Supersignal Westpico Chemiluminescent Substrate (Thermo Scientific, Pittsburgh, PA). Antibodies for p-TAK1, TAK, p-IKK α/β, IkB-α, p-JNK, JNK and AKT were obtained from Cell Signaling Technology (Boston, MA), antibodies for p-AKT and HSP90α/β were from Santa Cruz Biotechnology (Santa Cruz, CA) and the antibody for GPR120 was from Novus Biologicals (Littleton, CO).

Immunofluorescence staining The staining was done in cells cultured on coverslips in a 6 well plate. Briefly, cells were fixed in 4% formaldehyde in PBS, blocked with 5% normal goat serum, incubated with rabbit anti-NFκB p65 antibody (Cell signaling) followed by incubation with the Alexa Fluor 546 goat anti-rabbit antibody (Invitrogen) and mounted with Vectashield mounting medium with DAPI (Vector laboratories Inc., Burlingame, CA). The slides were examined under a fluorescence microscope.

Apoptosis Assay *Caspase-Glo 3/7 assay:* Following DHA treatment cells were subjected to Caspase 3 and 7 activity measurements using the Caspase-Glo assay kit (Promega). Briefly, a 96 well plate containing cells was removed from the incubator and allowed to equilibrate to room temperature for 30 minutes. 100 µl of Caspase-Glo reagent was added to each well and gently mixed with a plate shaker at 300–500 rpm for 30 seconds. The plate was then incubated at room temperature for 2 hours. The luminescence of each sample was measured in a plate-reading luminometer. The experiments were performed in triplicate and repeated on two separately

initiated cultures. *FITC Annexin V apoptosis assay*: Following DHA treatment cells were harvested and then stained with FITC Annexin V and Propidium iodide using the FITC Annexin V Apoptosis Detection Kit I (BD Biosciences) and following the manufacturer's protocol. The percentage of apoptotic cells was quantified by FACSCalibur Flow Cytometry (BD Biosciences).

Statistical Analyses. Data are presented as mean ± SEM. Differences between two groups was evaluated using Student's t-test and between multiple groups using analysis of variance followed by Bonferroni's, Tukey's or Dunnett's multiple comparisons post hoc tests. Tumor data were not normally distributed and were analyzed by the Kruskal-Wallis test followed by Dunn's multiple comparisons test or, in the case of a single comparison by the Mann-Whitney test. Tumor data are reported as box-whisker plots indicating the median, the first and third quartiles, and the 10^{th} and 90^{th} percentile. Pearson's correlation analysis was performed to test the association between body weight and tumor growth as well as between body weight and proinflammatory macrophage infiltration in the mammary fat pad. A p value < 0.05 was considered significant.

Conflict of interest

The authors declare no conflict of interest.

Acknowledgements

We thank Dr. Robert Cardiff for reviewing histologic sections of tumors and Hang Ha and Jonathan Hasselmann for assistance with animal maintenance. We thank the UCSD Histology Core lab for technical assistance with processing the tumor samples.

The study was funded in part by the National Institutes of Health grants U54 CA155435, P30 CA23100, P30 DK063491 (J.M.O.), K22 CA118182 (L.G.E.), the Department of Defense grant BC102147 (J.M.O.) and a Doris Howell Foundation Scholarship (J.T.S.).

Supplementary Information accompanies the paper on the Oncogene website

(http://www.nature.com/onc).

References

1 Biswas T, Gu X, Yang J, Ellies LG, Sun LZ. Attenuation of TGF-beta signaling supports tumor progression of a mesenchymal-like mammary tumor cell line in a syngeneic murine model. *Cancer letters* 2014; **346:** 129-138.

2 Calviello G, Su HM, Weylandt KH, Fasano E, Serini S, Cittadini A. Experimental evidence of omega-3 polyunsaturated fatty acid modulation of inflammatory cytokines and bioactive lipid mediators: their potential role in inflammatory, neurodegenerative, and neoplastic diseases. *BioMed research international* 2013; **2013:** 743171.

3 Cui LF, Guo XJ, Wei J, Liu FF, Fan Y, Lang RG *et al*. Overexpression of TNF-alpha and TNFRII in invasive micropapillary carcinoma of the breast: clinicopathological correlations. *Histopathology* 2008; **53:** 381-388.

4 de Lorgeril M, Salen P. New insights into the health effects of dietary saturated and omega-6 and omega-3 polyunsaturated fatty acids. *BMC medicine* 2012; **10:** 50.

5 Fares H, Lavie CJ, DiNicolantonio JJ, O'Keefe JH, Milani RV. Omega-3 fatty acids: a growing ocean of choices. *Current atherosclerosis reports* 2014; **16:** 389.

6 Golabek T, Bukowczan J, Chlosta P, Powroznik J, Dobruch J, Borowka A. Obesity and prostate cancer incidence and mortality: a systematic review of prospective cohort studies. *Urologia internationalis* 2014; **92:** 7-14.

7 Handgraaf S, Riant E, Fabre A, Waget A, Burcelin R, Liere P *et al*. Prevention of obesity and insulin resistance by estrogens requires ERalpha activation function-2 (ERalphaAF-2), whereas ERalphaAF-1 is dispensable. *Diabetes* 2013; **62:** 4098-4108.

8 Healy LA, Ryan AM, Carroll P, Ennis D, Crowley V, Boyle T *et al*. Metabolic syndrome, central obesity and insulin resistance are associated with adverse pathological features in postmenopausal breast cancer. *Clinical oncology* 2010; **22:** 281-288.

9 Iyengar NM, Hudis CA, Gucalp A. Omega-3 fatty acids for the prevention of breast cancer: an update and state of the science. *Current breast cancer reports* 2013; **5:** 247-254.

10 Jing K, Wu T, Lim K. Omega-3 polyunsaturated fatty acids and cancer. *Anti-cancer agents in medicinal chemistry* 2013; **13:** 1162-1177.

11 Kang KS, Wang P, Yamabe N, Fukui M, Jay T, Zhu BT. Docosahexaenoic acid induces apoptosis in MCF-7 cells in vitro and in vivo via reactive oxygen species formation and caspase 8 activation. *PloS one* 2010; **5:** e10296.

12 Khaw KT. Dietary fats and breast cancer risk. *Bmj* 2013; **347:** f4518.

13 Kolodecik T, Shugrue C, Ashat M, Thrower EC. Risk factors for pancreatic cancer: underlying mechanisms and potential targets. *Frontiers in physiology* 2013; **4:** 415.

14 Li P, Lu M, Nguyen MT, Bae EJ, Chapman J, Feng D *et al*. Functional heterogeneity of CD11c-positive adipose tissue macrophages in diet-induced obese mice. *The Journal of biological chemistry* 2010; **285:** 15333-15345.

15 Ligibel JA, Strickler HD. Obesity and its impact on breast cancer: tumor incidence, recurrence, survival, and possible interventions. *American Society of Clinical Oncology educational book / ASCO American Society of Clinical Oncology Meeting* 2013**:** 52-59.

16 Maccio A, Madeddu C. Obesity, inflammation, and postmenopausal breast cancer: therapeutic implications. *TheScientificWorldJournal* 2011; **11:** 2020-2036.

17 MacLennan MB, Clarke SE, Perez K, Wood GA, Muller WJ, Kang JX *et al*. Mammary tumor development is directly inhibited by lifelong n-3 polyunsaturated fatty acids. *The Journal of nutritional biochemistry* 2013; **24:** 388-395.

18 Manni A, Richie JP, Jr., Xu H, Washington S, Aliaga C, Bruggeman R *et al*. Influence of omega-3 fatty acids on Tamoxifen-induced suppression of rat mammary carcinogenesis. *International journal of cancer Journal international du cancer* 2014; **134:** 1549-1557.

19 Oh DY, Talukdar S, Bae EJ, Imamura T, Morinaga H, Fan W *et al*. GPR120 is an omega-3 fatty acid receptor mediating potent anti-inflammatory and insulin-sensitizing effects. *Cell* 2010; **142:** 687-698.

20 Olefsky JM, Glass CK. Macrophages, inflammation, and insulin resistance. *Annual review of physiology* 2010; **72:** 219-246.

21 Parada B, Reis F, Cerejo R, Garrido P, Sereno J, Xavier-Cunha M *et al*. Omega-3 fatty acids inhibit tumor growth in a rat model of bladder cancer. *BioMed research international* 2013; **2013:** 368178.

22 Patterson RE, Rock CL, Kerr J, Natarajan L, Marshall SJ, Pakiz B *et al*. Metabolism and breast cancer risk: frontiers in research and practice. *Journal of the Academy of Nutrition and Dietetics* 2013; **113:** 288-296.

23 Ramos-Nino ME. The role of chronic inflammation in obesity-associated cancers. *ISRN oncology* 2013; **2013:** 697521.

24 Rose DP, Vona-Davis L. Influence of obesity on breast cancer receptor status and prognosis. *Expert review of anticancer therapy* 2009; **9:** 1091-1101.

25 Sczaniecka AK, Brasky TM, Lampe JW, Patterson RE, White E. Dietary intake of specific fatty acids and breast cancer risk among postmenopausal women in the VITAL cohort. *Nutrition and cancer* 2012; **64:** 1131-1142.

26 Seki E, Brenner DA, Karin M. A liver full of JNK: signaling in regulation of cell function and disease pathogenesis, and clinical approaches. *Gastroenterology* 2012; **143:** 307-320.

27 Sheen-Chen SM, Chen WJ, Eng HL, Chou FF. Serum concentration of tumor necrosis factor in patients with breast cancer. *Breast cancer research and treatment* 1997; **43:** 211-215.

28 Signori C, El-Bayoumy K, Russo J, Thompson HJ, Richie JP, Hartman TJ *et al*. Chemoprevention of breast cancer by fish oil in preclinical models: trials and tribulations. *Cancer research* 2011; **71:** 6091-6096.

29 Simopoulos AP. Genetic variants in the metabolism of omega-6 and omega-3 fatty acids: their role in the determination of nutritional requirements and chronic disease risk. *Experimental biology and medicine* 2010; **235:** 785-795.

30 Simpson ER, Brown KA. Minireview: Obesity and breast cancer: a tale of inflammation and dysregulated metabolism. *Molecular endocrinology* 2013; **27:** 715-725.

31 Subbaramaiah K, Howe LR, Bhardwaj P, Du B, Gravaghi C, Yantiss RK *et al*. Obesity is associated with inflammation and elevated aromatase expression in the mouse mammary gland. *Cancer prevention research* 2011; **4:** 329-346.

32 Sundaram S, Johnson AR, Makowski L. Obesity, metabolism and the microenvironment: Links to cancer. *Journal of carcinogenesis* 2013; **12:** 19.

33 van Kruijsdijk RC, van der Wall E, Visseren FL. Obesity and cancer: the role of dysfunctional adipose tissue. *Cancer epidemiology, biomarkers & prevention : a publication of the American Association for Cancer Research, cosponsored by the American Society of Preventive Oncology* 2009; **18:** 2569-2578.

34 Wong SW, Kwon MJ, Choi AM, Kim HP, Nakahira K, Hwang DH. Fatty acids modulate Toll-like receptor 4 activation through regulation of receptor dimerization and recruitment into lipid rafts in a reactive oxygen species-dependent manner. *The Journal of biological chemistry* 2009; **284:** 27384-27392.

35 Wu Q, Wang H, Zhao X, Shi Y, Jin M, Wan B *et al*. Identification of G-protein-coupled receptor 120 as a tumor-promoting receptor that induces angiogenesis and migration in human colorectal carcinoma. *Oncogene* 2013; **32:** 5541-5550.

36 Xue M, Wang Q, Zhao J, Dong L, Ge Y, Hou L *et al*. Docosahexaenoic acid inhibited the Wnt/beta-catenin pathway and suppressed breast cancer cells in vitro and in vivo. *The Journal of nutritional biochemistry* 2014; **25:** 104-110.

37 Zheng JS, Hu XJ, Zhao YM, Yang J, Li D. Intake of fish and marine n-3 polyunsaturated fatty acids and risk of breast cancer: meta-analysis of data from 21 independent prospective cohort studies. *Bmj* 2013; **346:** f3706.

Figure legends

Figure 1. HFD-induced obesity and genetic obesity promote mammary tumor growth. OVX WT, Het (+/ob) and ob/ob mice were fed NC or a HFD. **A:** Body weights of mice were measured weekly from the start of NC or HFD feeding (0 wk) to the study end (15 wk). Body weights are shown at 0, 8, and 15 weeks. n=7-10 mice per group. Data are expressed as mean ± SEM, *$p < 0.05$ vs WT, Het or ob/ob mice on NC, $^{\#}p < 0.05$ vs. WT or Het mice on HFD. **B:** Py230 cells were injected into the mammary fat pads after eight weeks of HFD and tumor burden was measured at seven weeks after tumor cell injection. n=7-10 mice per group. Data are expressed as 10-90 percentile, *$p < 0.001$ WT NC vs. WT HFD; Het NC vs. Het HFD; Het NC vs. ob/ob NC; Het NC vs. ob/ob HFD, $^{\#}p < 0.05$ Het HFD vs ob/ob HFD. **C:** The weights of mammary tumors (n=220) collected from all the mice were plotted against the body weights of corresponding mice.

Figure 2. Inflammatory macrophage infiltration and inflammatory cytokine gene expression are increased in the mammary fat pad of HFD-induced and genetically obese mice. A and B: Stromal vascular cells (SVCs) were isolated from the mammary fat pads, stained with F4/80, CD11b, and CD11c antibodies and analyzed by FACS. HFD-fed WT and Het mice, NC-fed ob/ob and HFD-fed ob/ob mice showed significantly higher expression of triple positive M1-like macrophages in the mammary fat pads than NC-fed WT and Het mice (*$p < 0.05$). M1-type macrophage population (% of total macrophages) = $(F4/80^{+}CD11b^{+}CD11c^{+})/(F4/80^{+}CD11b^{+}) \times 100$. n=5-7 per group. Data are expressed as mean ± SEM. **C:** The calculated M1 population (%) from all the mice (n=36) was plotted against the body weights of corresponding mice. **D:** The mRNA levels for MCP-1and TNF-α in the

mammary fat pads were determined by qPCR. n=6-8 per group. Data are expressed as mean ± SEM, *p < 0.05 vs. WT or Het on NC.

Figure 3. TNF-α enhances Py230 cell proliferation and activates NFκB and JNK signaling *in vitro*. **A:** Py230 cells were treated with vehicle or different concentrations of TNF-α or MCP-1 and cultured in 24 well plates for 9 days. Cell growth was determined by counting cell number on Day 3, 6 and 9. Data are expressed as mean ± SEM of duplicate samples at each time point combined from two independent experiments. *p < 0.05 control vs. 5, 10 ng/ml TNF-α treated, **p<0.01 control vs. 1, 5, 10 ng/ml TNF-α treated. **B:** Py230 cells were pretreated with vehicle, JNK inhibitor, or NFκB inhibitor for 30 min and then treated with or without TNF-α and cultured for 4 or 5 days. Treatments were refreshed every day and cell growth was determined after 72 or 96 hr. Data represent 3 independent experiments and are expressed as means ± SEM. $^{*}p < 0.05$ vs. vehicle, $^{**}p < 0.001$ vs. vehicle, $^{\#}p < 0.001$ vs. TNF-α, $^{\#\#}p < 0.001$ vs. NFkB inhibitor. **C:** Representative western blot of Py230 cells treated with TNF-α (10 ng/ml) for 10 min and blotted for JNK, TAK1 and IKK phosphorylation or IKB-α levels. **D:** Quantification of western blot data from 3 independent experiments. Data are presented as mean ± SEM, *p < 0.05 vs. vehicle.

Figure 4. Macrophage and inflammatory cytokine gene expression in perigonadal fat and the mammary fat pad of HFD or FOD-fed mice in the absence of tumor cell injection. The mRNA levels for the macrophage marker F4/80, M-1type macrophage marker CD11c and inflammatory cytokines were determined by qPCR. **A:** Perigonadal fat **B:** Mammary fat pad. n=8 per group. Data are expressed as mean ± SEM, *p < 0.05 vs. HFD.

Figure 5. FOD significantly reduces mammary tumor growth in both WT and GPR120 KO mice and tumor cell injection modulates inflammation in the mammary fat pad and perigonadal fat. **A:** OVX WT mice were fed a HFD for four weeks and then either switched to a FOD or maintained on the HFD. Py230 cells were injected into the mammary fat pads at 14 weeks after starting the HFD and tumor burden was measured at 8 weeks after tumor cell injection (22 total weeks of diet protocol, n=16 tumors per group). *$p < 0.05$ vs. HFD. **B:** The mRNA levels for GPR120 in mammary tumors and the mammary fat pad of HFD- and FOD-fed mice were determined by qPCR. n= 5-8 per group. Data are expressed as mean ± SEM, ***$p < 0.001$ vs. tumor. GPR120 protein expression was determined in the mammary fat pads of 3 mice (lanes 2-4) and matching mammary tumors (lanes 5-7) from HFD-fed mice by Western blotting. Lane 1 is the positive control, (PC): 293 cells expressing exogenous GPR120. **C, D:** Macrophage and inflammatory cytokine gene expression in the mammary fat pad (**C**) and perigonadal fat (**D**) of HFD or FOD-fed mice bearing tumors. The mRNA levels for genes were determined by qPCR. n=6-8 per group. Data are expressed as mean ± SEM, *$p < 0.05$ vs. HFD. **E, F:** OVX WT mice were fed a HFD. One group of tumor naïve mice and another group of mice bearing Py230 mammary tumors were dissected at 20 weeks after starting HFD feeding. The mRNA levels for F4/80, CD11c, MCP-1, TNF-α, IL-6, IL-1β, iNOS and Arg-1 in the mammary fat pad (**E**) and perigonadal fat (**F**) of mice were determined by qPCR. TCI: tumor cell injection. n= 5-8 per group. Data are expressed as mean ± SEM, *$p < 0.05$ vs. no TCI. **G:** OVX GPR120 KO mice were fed a HFD for four weeks and then switched to a FOD or maintained on a HFD. Py230 tumor cell injection was performed after 13 weeks after HFD feeding and tumor burden was determined at 7 weeks after tumor cell injection (20 total weeks of diet, n= 24-28 tumors per group). *$p < 0.05$ vs. HFD.

Figure 6. Effect of ω-3 PUFAs on cell growth, signaling and apoptosis in Py230 cells.

A: Py230 WT and PyVmT/GPR120 KO cells were treated with different concentrations of DHA for 48 hr before performing the MTT assay. Relative cell viability is expressed as a percentage of the control that was not treated with DHA. Data are expressed as mean ± SEM, * $p < 0.01$ vs. vehicle. **B:** Cells were pretreated with vehicle or DHA (40 μM) for 1 hr and then treated with or without TNF-α. DHA/TNF-α treatment was refreshed every day and cell growth was determined after 72 hr. Data are expressed as mean ± SEM, * $p < 0.001$ vs. vehicle, $^{\#}p < 0.01$ vs. vehicle. **C:** Py230 cells were treated with vehicle or DHA (100 μM) for 1 hr prior to treatment with vehicle, TNF-α (10 ng/ml) for 10 min or LPS (100 ng/ml) for 15 min and then cell lysates were prepared and subjected to Western blotting. **D:** Py230 cells were treated with vehicle or DHA for 7 or 24 hr and caspase 3/7 activity was measured. Data are expressed as mean ± SEM, ***$p < 0.001$ vs. vehicle. **E:** Py230 cells were treated with vehicle or DHA for 48 hr and FITC Annexin V staining was performed to determine early and late apoptosis by FACS. Data represent two independent experiments and are expressed as mean ± SEM, ***$p < 0.001$ vs. vehicle. **F:** Representative western blot of Py230 cells treated with vehicle or DHA (100 μM) for 1 hr prior to treatment with vehicle or insulin (10 nM) for 10 min and blotted for AKT and JNK phosphorylation. Quantification of western blot data from 3 independent experiments. Data are presented as mean ± SEM, *$p < 0.05$ vs. vehicle or insulin alone.

Figure 1.

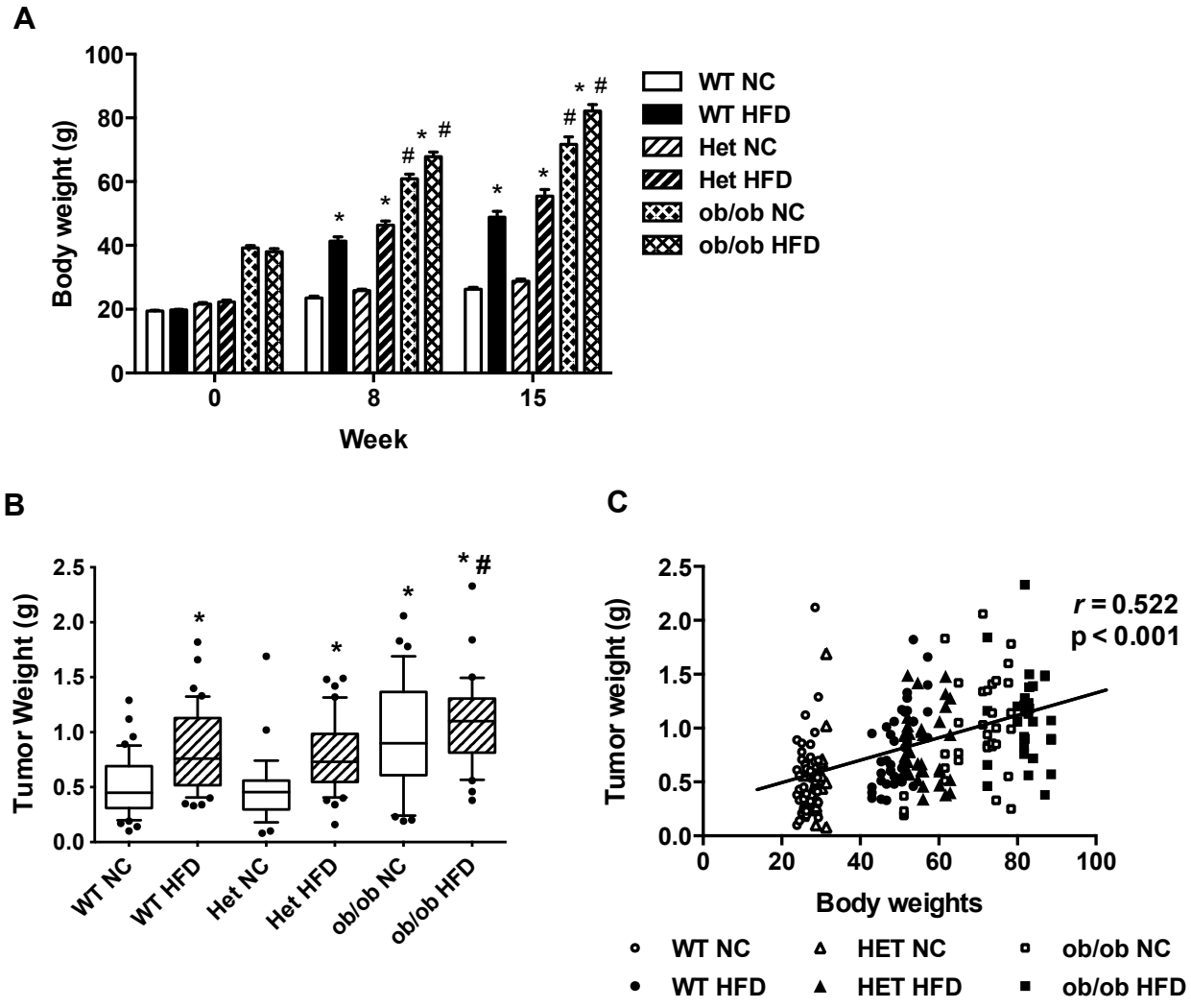
A
Body weight (g)
Week
WT NC
WT HFD
Het NC
Het HFD
ob/ob NC
ob/ob HFD
B
Tumor Weight (g)
WT NC
WT HFD
Het NC
Het HFD
ob/ob NC
ob/ob HFD
C
Tumor weight (g)
Body weights
r = 0.522
p < 0.001
WT NC
WT HFD
HET NC
HET HFD
ob/ob NC
ob/ob HFD

Figure 2.

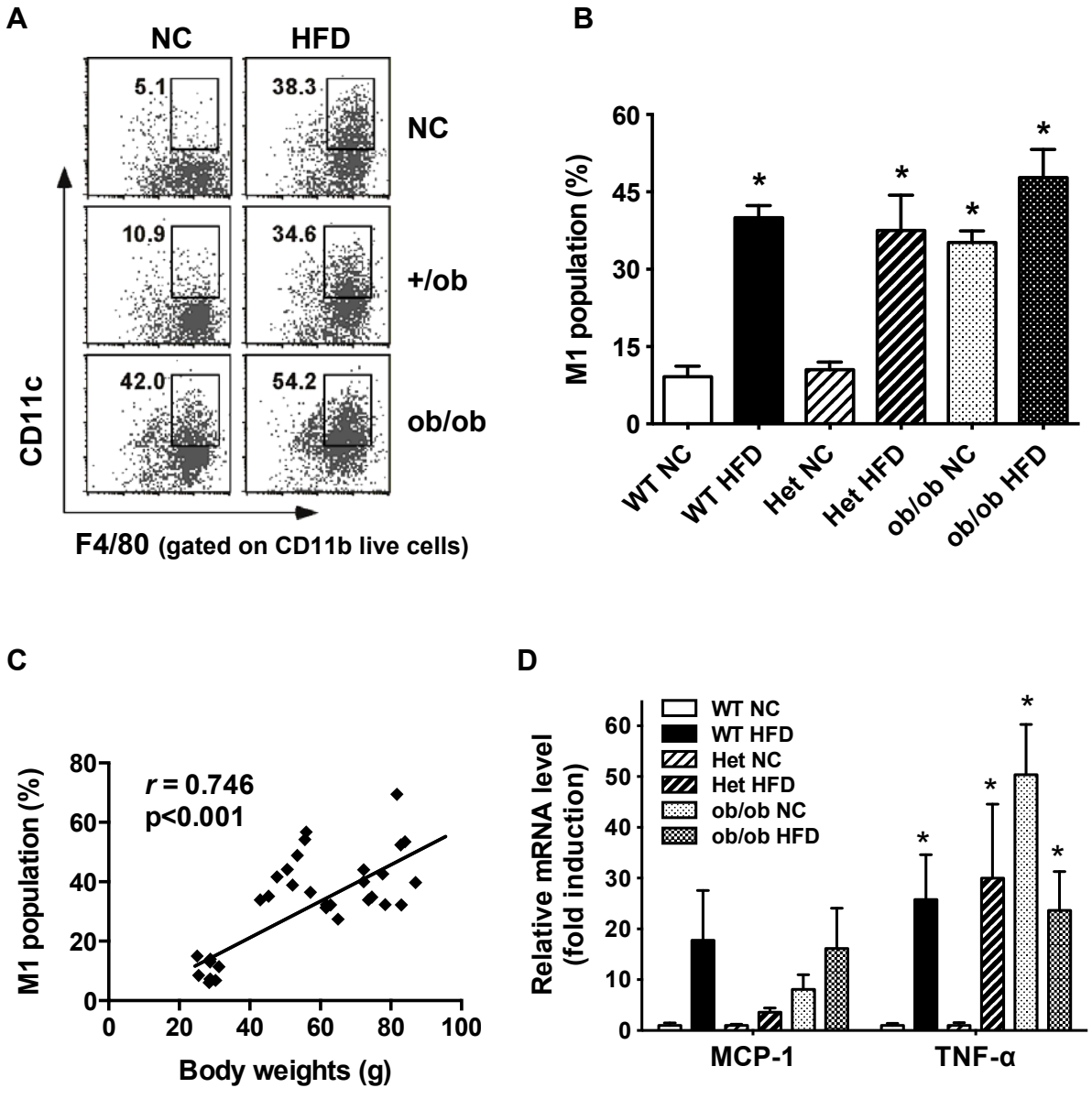
A
NC
HFD
5.1
38.3
NC
10.9
34.6
+/ob
42.0
54.2
ob/ob
CD11c
F4/80 (gated on CD11b live cells)
B
M1 population (%)
60
45
30
15
0
WT NC
WT HFD
Het NC
Het HFD
ob/ob NC
ob/ob HFD
C
M1 population (%)
r = 0.746
p<0.001
80
60
40
20
0
0
20
40
60
80
100
Body weights (g)
D
Relative mRNA level (fold induction)
WT NC
WT HFD
Het NC
Het HFD
ob/ob NC
ob/ob HFD
60
50
40
30
20
10
0
MCP-1
TNF-α

Figure 3.

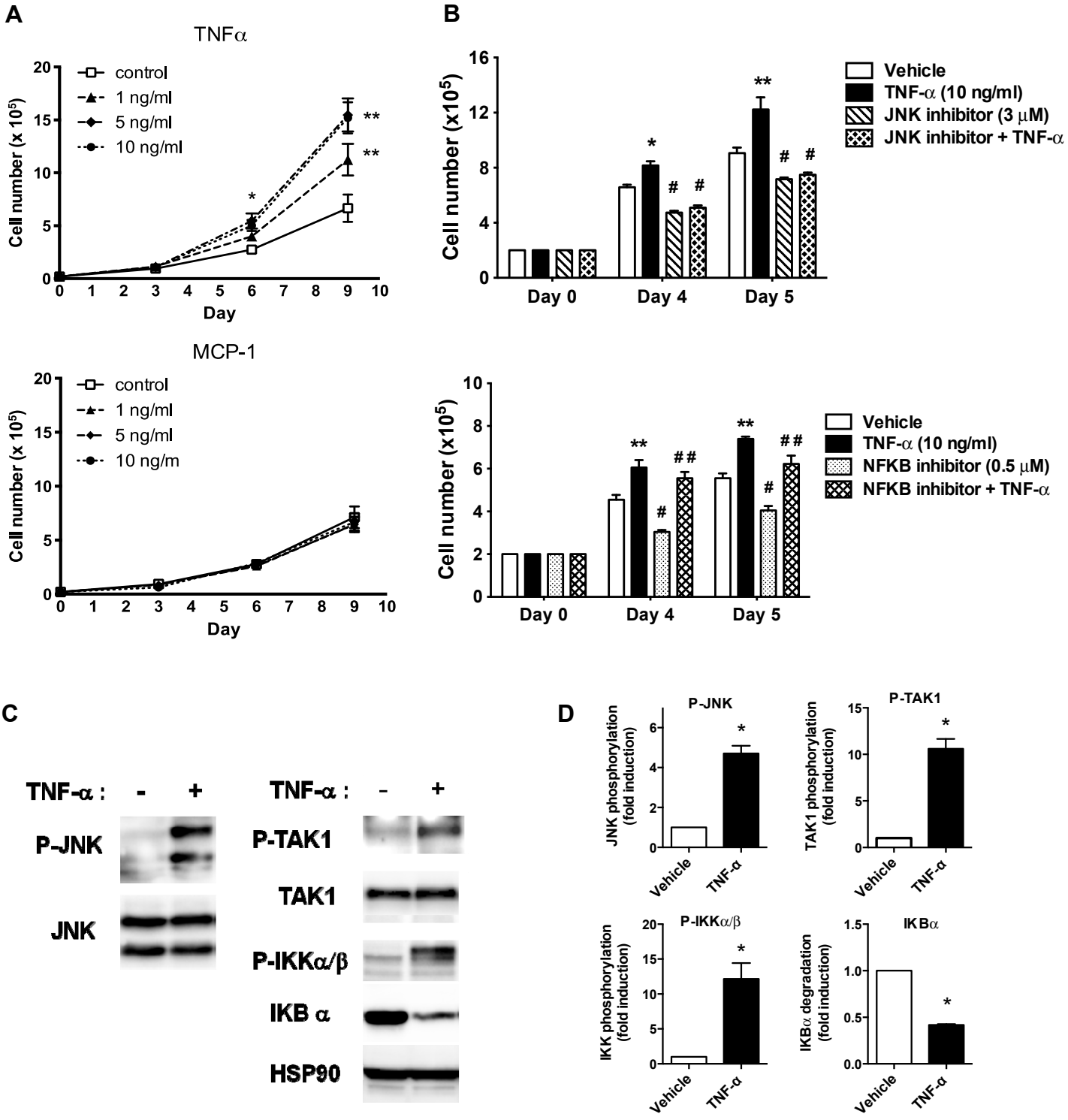
A
TNFα
control
1 ng/ml
5 ng/ml
10 ng/ml
Cell number (x 10^5)
Day
MCP-1
control
1 ng/ml
5 ng/ml
10 ng/m
Cell number (x 10^5)
Day
B
Cell number (x10^5)
Vehicle
TNF-α (10 ng/ml)
JNK inhibitor (3 μM)
JNK inhibitor + TNF-α
Day 0
Day 4
Day 5
Cell number (x10^5)
Vehicle
TNF-α (10 ng/ml)
NFKB inhibitor (0.5 μM)
NFKB inhibitor + TNF-α
Day 0
Day 4
Day 5
C
TNF-α : - +
P-JNK
JNK
TNF-α : - +
P-TAK1
TAK1
P-IKKα/β
IKB α
HSP90
D
P-JNK
JNK phosphorylation (fold induction)
Vehicle
TNF-α
P-TAK1
TAK1 phosphorylation (fold induction)
Vehicle
TNF-α
P-IKKα/β
IKK phosphorylation (fold induction)
Vehicle
TNF-α
IKBα
IKBα degradation (fold induction)
Vehicle
TNF-α

Figure 4.

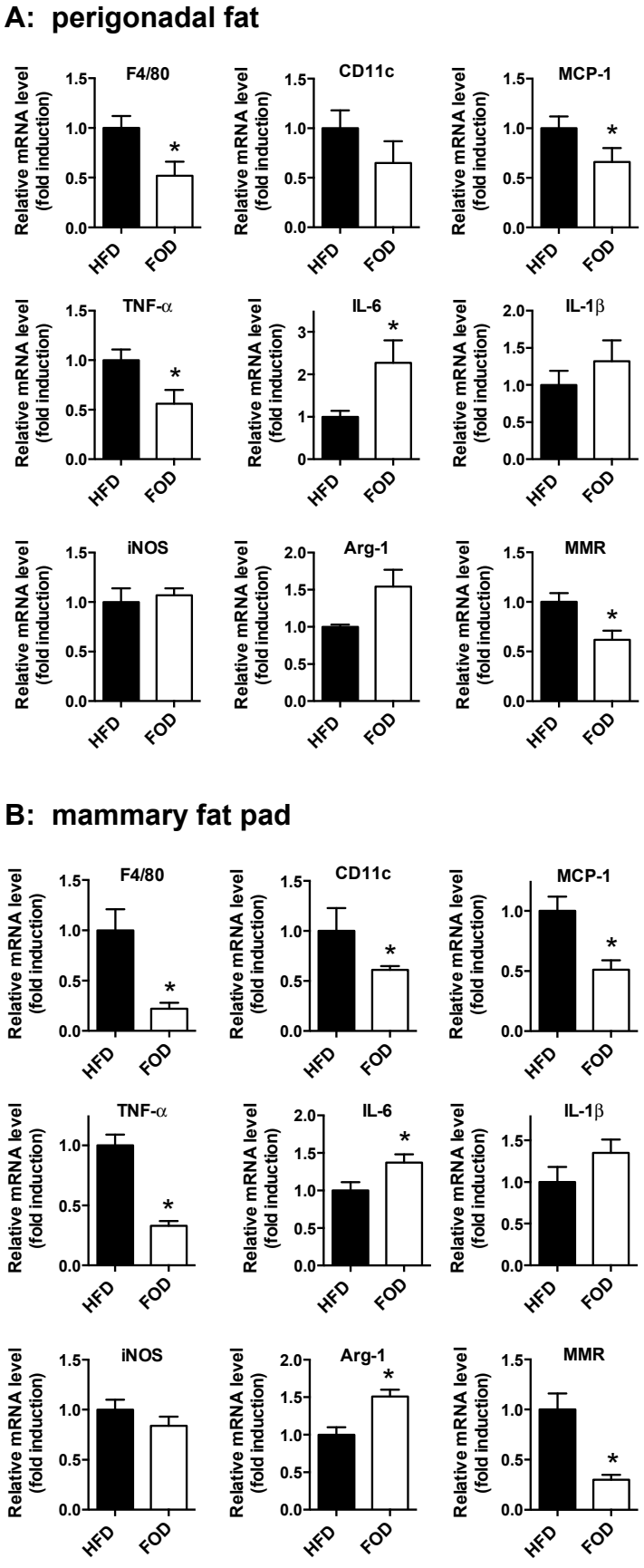
A: perigonadal fat
F4/80
CD11c
MCP-1
TNF-α
IL-6
IL-1β
iNOS
Arg-1
MMR
Relative mRNA level (fold induction)
HFD
FOD
B: mammary fat pad
F4/80
CD11c
MCP-1
TNF-α
IL-6
IL-1β
iNOS
Arg-1
MMR
Relative mRNA level (fold induction)
HFD
FOD

Figure 5.

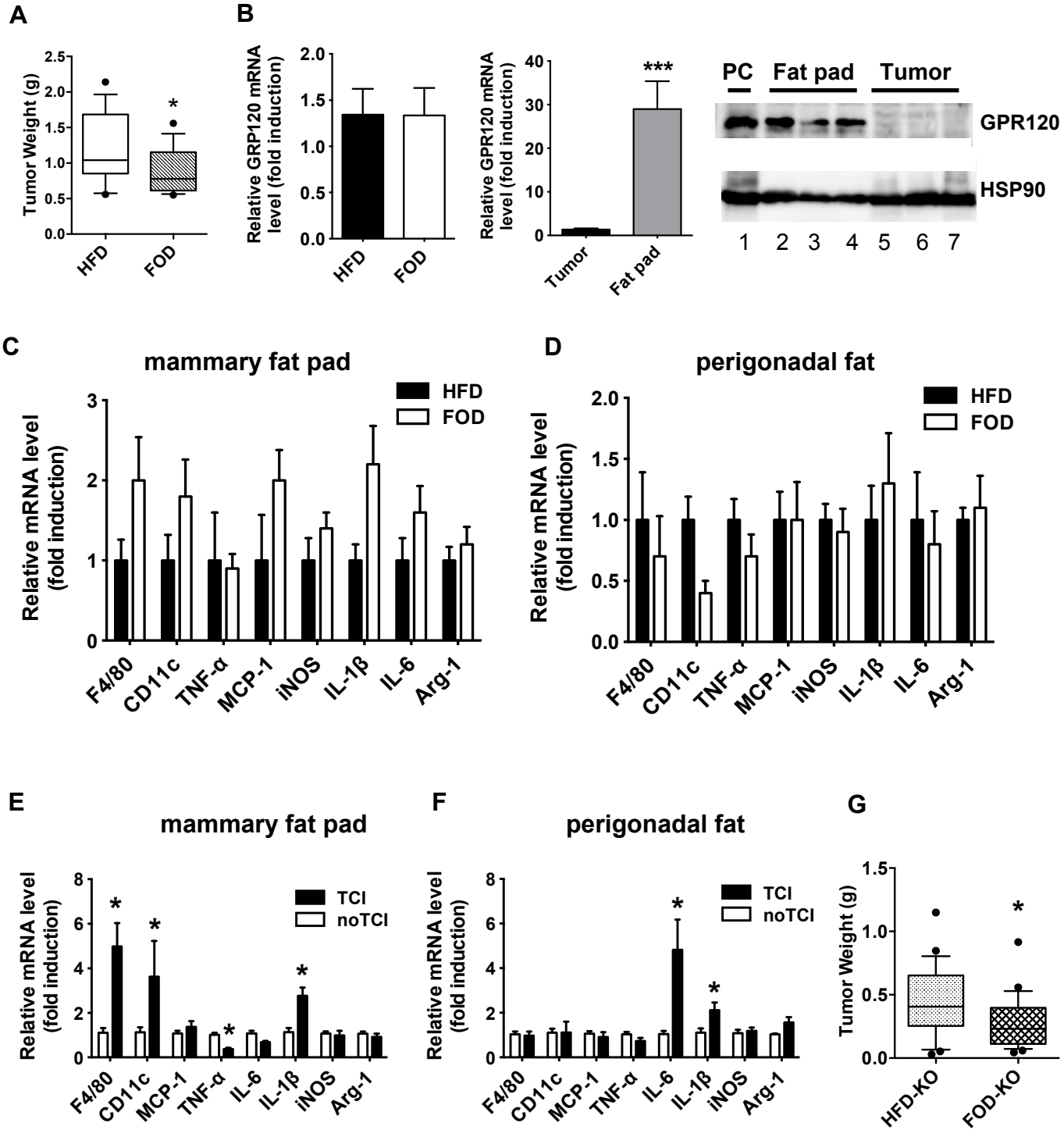
A
Tumor Weight (g)
HFD
FOD
B
Relative GRP120 mRNA level (fold induction)
HFD
FOD
Relative GPR120 mRNA level (fold induction)
Tumor
Fat pad
PC
Fat pad
Tumor
GPR120
HSP90
1 2 3 4 5 6 7
C
mammary fat pad
HFD
FOD
Relative mRNA level (fold induction)
F4/80
CD11c
TNF-α
MCP-1
iNOS
IL-1β
IL-6
Arg-1
D
perigonadal fat
HFD
FOD
Relative mRNA level (fold induction)
F4/80
CD11c
TNF-α
MCP-1
iNOS
IL-1β
IL-6
Arg-1
E
mammary fat pad
TCI
noTCI
Relative mRNA level (fold induction)
F4/80
CD11c
MCP-1
TNF-α
IL-6
IL-1β
iNOS
Arg-1
F
perigonadal fat
TCI
noTCI
Relative mRNA level (fold induction)
F4/80
CD11c
MCP-1
TNF-α
IL-6
IL-1β
iNOS
Arg-1
G
Tumor Weight (g)
HFD-KO
FOD-KO

Figure 6.

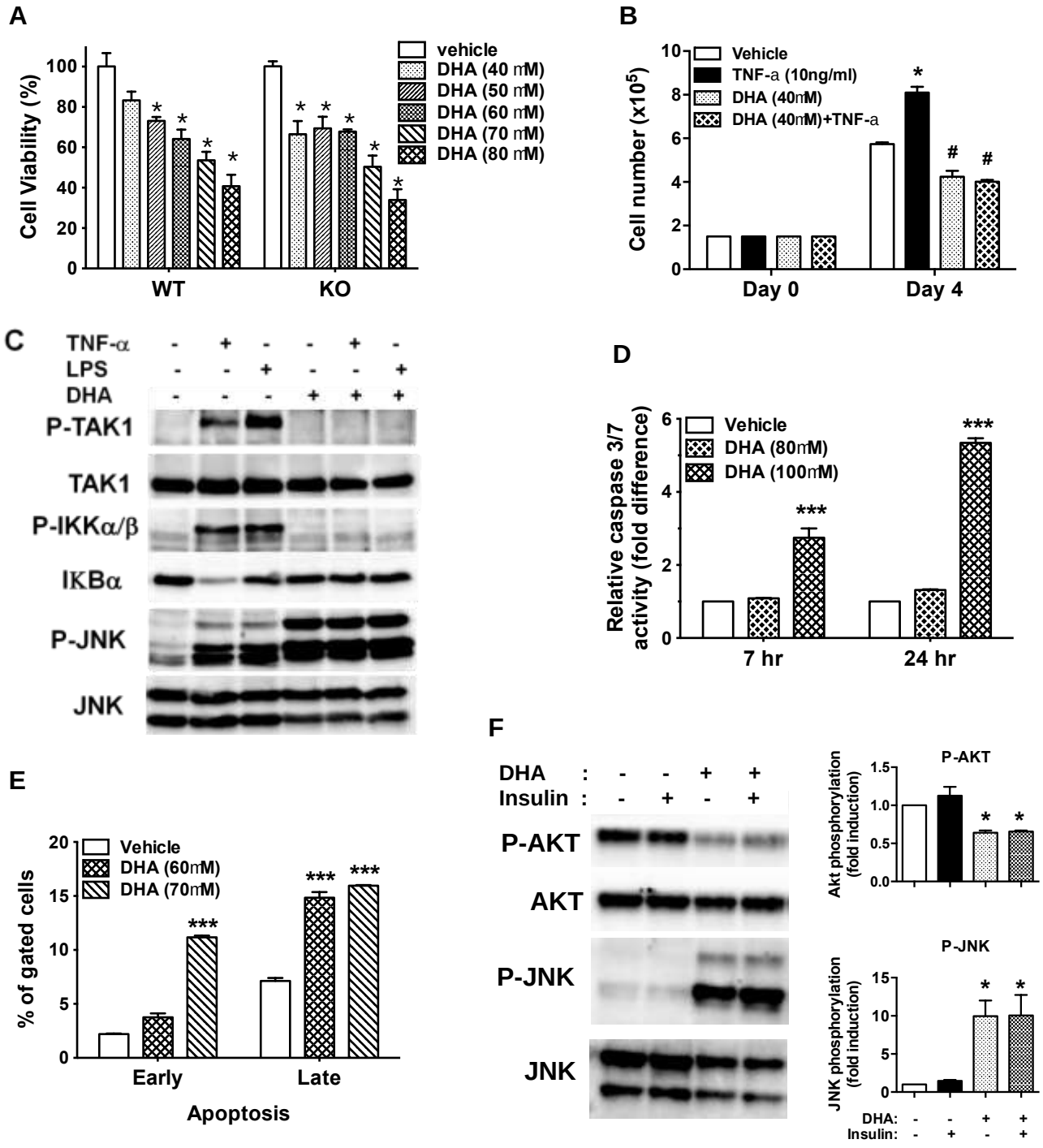
A
Cell Viability (%)
vehicle
DHA (40 mM)
DHA (50 mM)
DHA (60 mM)
DHA (70 mM)
DHA (80 mM)
WT
KO
B
Cell number (x10^5)
Vehicle
TNF-a (10ng/ml)
DHA (40mM)
DHA (40mM)+TNF-a
Day 0
Day 4
C
TNF-α
LPS
DHA
P-TAK1
TAK1
P-IKKα/β
IκBα
P-JNK
JNK
D
Relative caspase 3/7 activity (fold difference)
Vehicle
DHA (80mM)
DHA (100mM)
7 hr
24 hr
E
% of gated cells
Vehicle
DHA (60mM)
DHA (70mM)
Early
Late
Apoptosis
F
DHA :
Insulin :
P-AKT
AKT
P-JNK
JNK
Akt phosphorylation (fold induction)
JNK phosphorylation (fold induction)

Supplemental figures and Table

Figure S1. HFD-induced obesity and genetic obesity increase mammary fat depots. Mammary fat pad weights of mice were measured at the end of the study (15 wk). n=7-10 mice per group. Fat pad weights were expressed as a percentage of body weights. Data are expressed as means ± SEM, *$p < 0.05$ vs. WT or Het mice on NC, $^{\#}p < 0.05$ vs. WT or Het mice on HFD.

Figure S2. Proinflammatory cytokine expression in the mammary fat pads from lean and obese mice. The mRNA levels for IL-1β, IL-6 and iNOS in the mammary fat pads were determined by qPCR. n=6-8 per group. Data are expressed as means ± SEM. No significant differences between groups were observed.

Figure S3. M2-type macrophage associated anti-inflammatory gene expression in the mammary fat pads from lean and obese mice. The mRNA levels for Arg-1 and MGL-1 in the mammary fat pad were determined by qPCR. n=6-8 per group. Data are expressed as mean ± SEM. No significant differences between groups were observed.

Figure S4. Proinflammatory cytokine expression in mammary tumors from lean and obese mice. Mammary tumor lysates were subjected to a Luminex mouse cytokine 5-plex assay following a manufacture's instruction (Millipore). KC, MCP-1, IL-1β, IL-6 and TNF-α expression was measured in tumors. n=5-6 per group. Data are expressed as mean ± SEM. No significant differences between groups were observed.

Figure S5. Body weights of mice fed HFD or FOD. Body weights of mice measured at the start of HFD feeding (0 wk), after 14 wk, and the end of the study (22 wk). Py230 cells were injected into the mammary fat pads at 14 weeks after starting HFD (14 wk). All mice were fed with HFD

for the first 4 weeks and then half of the mice were switched to a FOD to the end of the study. n=4 per group. No significant differences between groups were observed.

Figure S6. Mammary tumor inflammation in mice fed HFD or FOD. The mRNA levels for F4/80, CD11c, TNF-α, iNOS, MCP-1, IL-1β, IL-6, Arg-1 and MMR in mammary tumors of HFD- fed and FOD-fed mice were determined by q-PCR. n=8 tumors per group. Data are expressed as mean ± SEM. No significant differences between groups were observed.

Figure S7. DHA prevents TNF-α and LPS-induced nuclear translocation of NFκB p65. Py230 cells were treated with vehicle or DHA (100 μM) for 1 hr prior to treatment with vehicle, TNF-α (10 ng/ml) for 10 min or LPS (100 ng/ml) for 15 min. Py230 cells were then fixed and stained with NFκB p65 antibody (red). Nuclei were stained with DAPI (blue).

Figure S1.

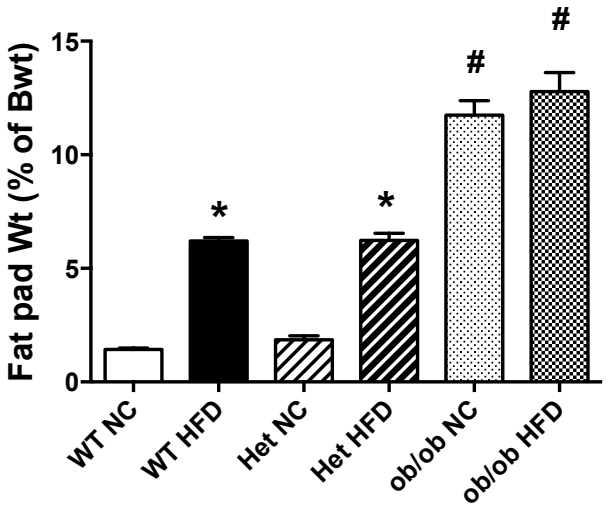
Fat pad Wt (% of Bwt)
15
10
5
0
*
*
#
#
WT NC
WT HFD
Het NC
Het HFD
ob/ob NC
ob/ob HFD

Figure S2.

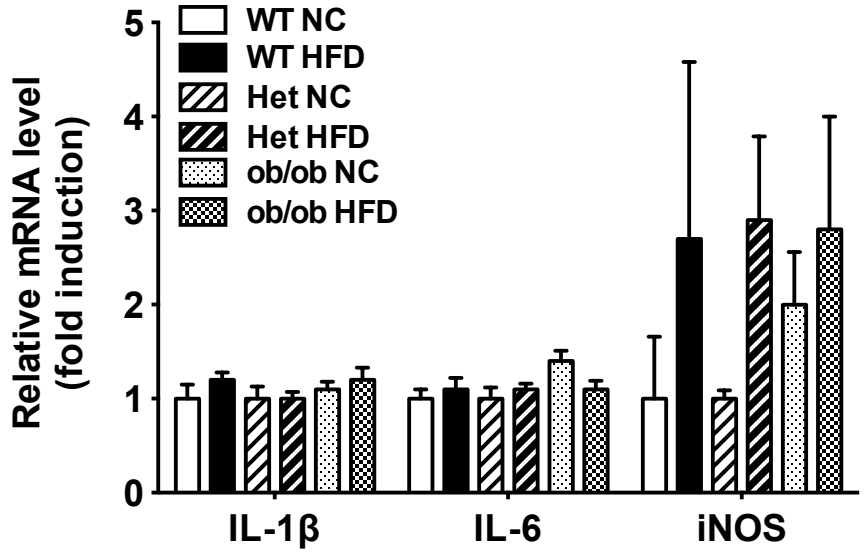
WT NC
WT HFD
Het NC
Het HFD
ob/ob NC
ob/ob HFD
Relative mRNA level
(fold induction)
0
1
2
3
4
5
IL-1β
IL-6
iNOS

Figure S3.

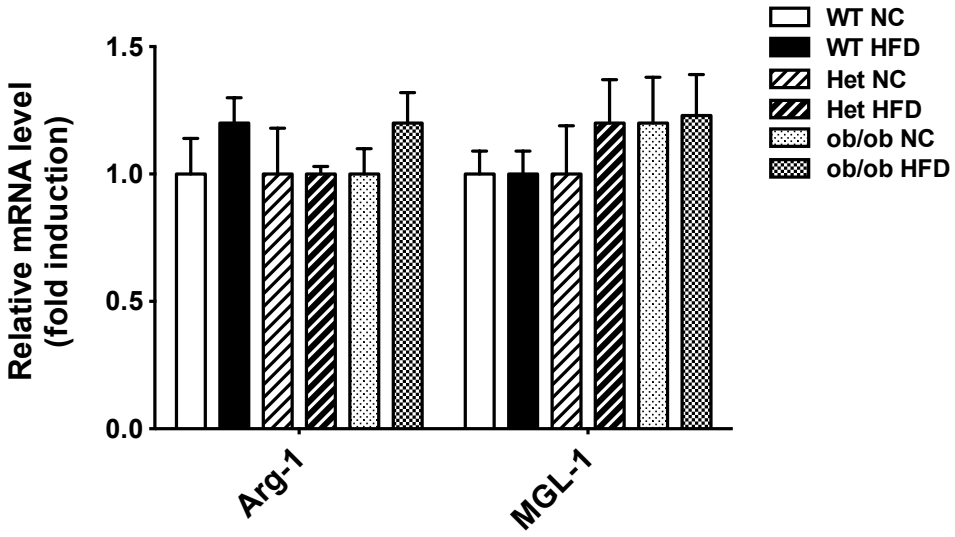
Relative mRNA level
(fold induction)
1.5
1.0
0.5
0.0
Arg-1
MGL-1
WT NC
WT HFD
Het NC
Het HFD
ob/ob NC
ob/ob HFD

Figure S4.

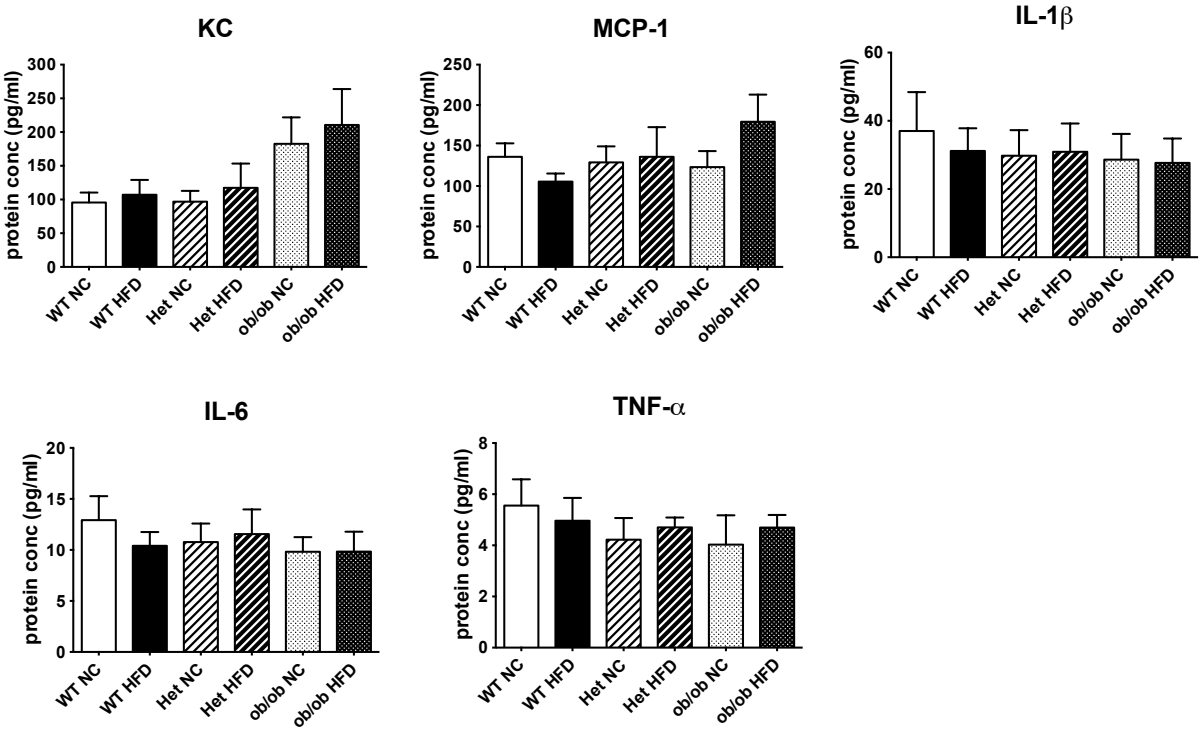
KC
protein conc (pg/ml)
300
250
200
150
100
50
0
WT NC
WT HFD
Het NC
Het HFD
ob/ob NC
ob/ob HFD
MCP-1
protein conc (pg/ml)
250
200
150
100
50
0
WT NC
WT HFD
Het NC
Het HFD
ob/ob NC
ob/ob HFD
IL-1β
protein conc (pg/ml)
60
40
20
0
WT NC
WT HFD
Het NC
Het HFD
ob/ob NC
ob/ob HFD
IL-6
protein conc (pg/ml)
20
15
10
5
0
WT NC
WT HFD
Het NC
Het HFD
ob/ob NC
ob/ob HFD
TNF-α
protein conc (pg/ml)
8
6
4
2
0
WT NC
WT HFD
Het NC
Het HFD
ob/ob NC
ob/ob HFD

Figure S5.

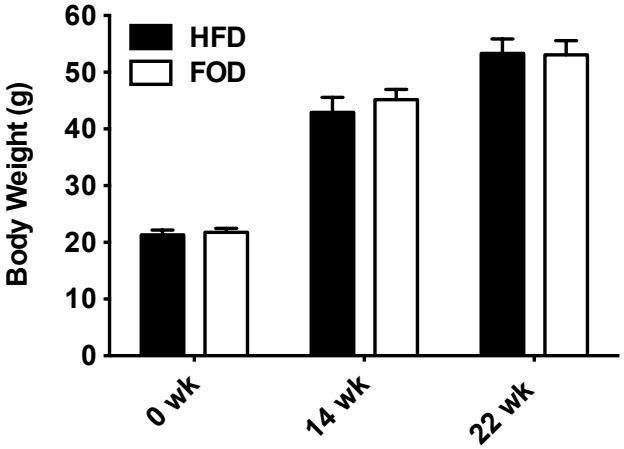

Figure S6.

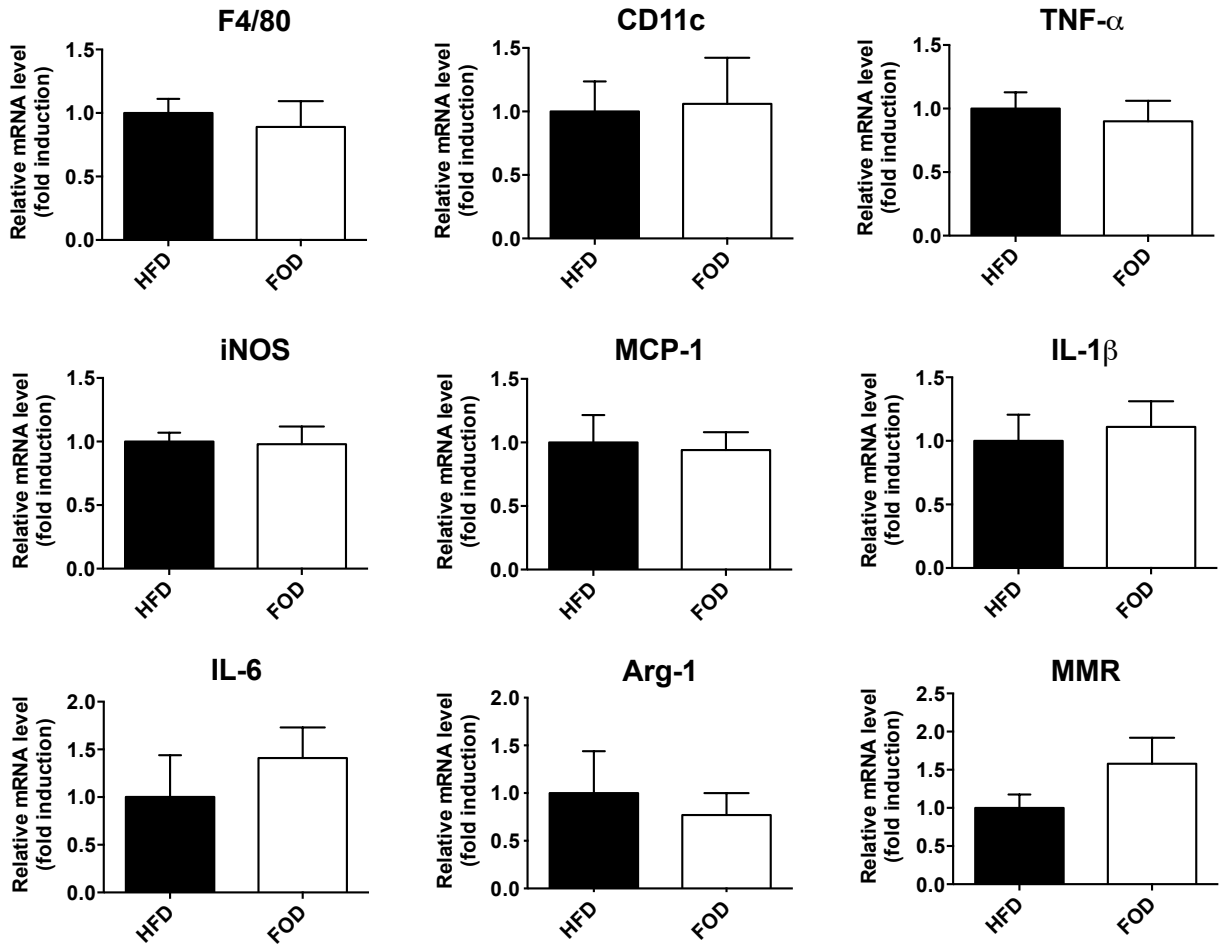
F4/80
CD11c
TNF-α
iNOS
MCP-1
IL-1β
IL-6
Arg-1
MMR
Relative mRNA level (fold induction)
HFD
FOD

Figure S7.

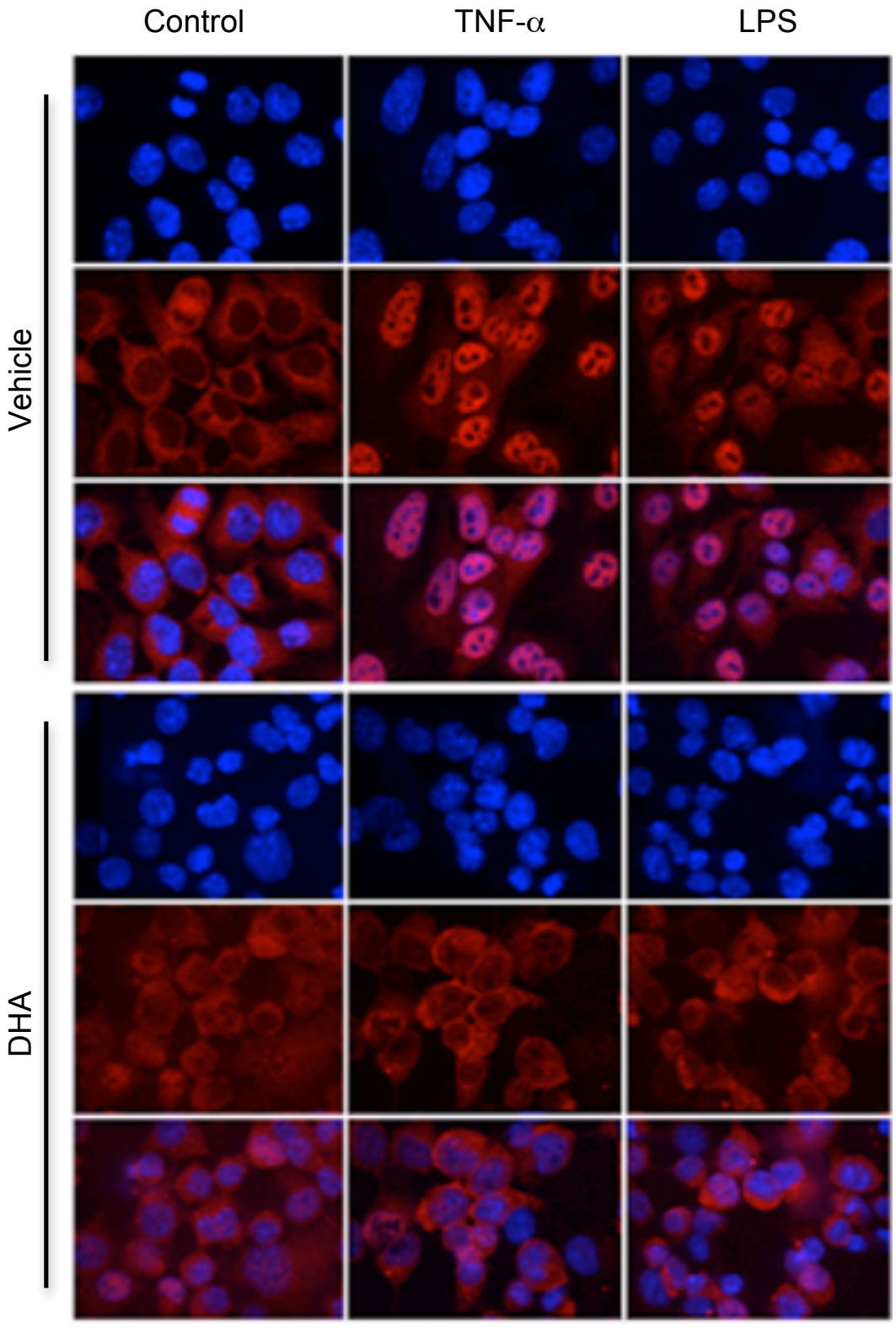

Table S1. Primer sequences for Q-PCR

Gene	Sequence
F4/80	F: 5'-CTTTGGCTATGGGCTTCCAGTC-3’ R: 5'-GCAAGGAGGACAGAGTTTATCGTG-3'
CD11c	F: 5'-ACGTCAGTACAAGGAGATGTTGGA-3' R: 5'-ATCCTATTGCAGAATGCTTCTTTACC -3'
TNF-α	F: 5'-CCAGACCCTCACACTCAGATC-3' R: 5'-CACTTGGTGGTTTGCTACGAC-3'
MCP-1	F: 5'-TCTGGACCCATTCCTTCTTG-3' R: 5'-AGGTCCCTGTCATGCTTCTG-3'
IL-1β	F: 5’-AAGGGCTGCTTCCAAACCTTTGAC-3' R: 5’-ATACTGCCTGCCTGAAGCTCTTGT-3'
IL-6	F: 5'-ATCCAGTTGCCTTCTTGGGACTGA-3' R: 5’-TAAGCCTCCGACTTGTGAAGTGGT-3'
iNOS	F: 5'-AATCTTGGAGCGAGTTGTGG-3' R: 5'-CAGGAAGTAGGTGAGGGCTTG-3'
Arg-1	F: 5'-TGGCTTTAACCTTGGCTTGCTTCG-3' R: 5'-CATGTGGCGCATTCACAGTCACTT-3'
MGL-1	F: 5'-ATGATGTCTGCCAGAGAACC-3' R: 5'-ATCACAGATTTCAGCAACCTTA-3'
MMR-1	F: 5'-CTCGTGGATCTCCGTGACAC-3' R: 5'-GCAAATGGAGCCGTCTGTGC-3'
GPR120	F: 5'-TACAGATCACGAAAGCATCGCGGA-3’ R: 5’- TGCGGAAGAGTCGGTAGTCTTGTT-3'
GAPDH	F: 5'-TCACCACCATGGAGAAGGC-3’ R: 5’-GCTAAGCAGTTGGTGGTGCA-3'
RPII	F: 5'-GATCAACAATCAGCTGCGGCGG-3’ R: 5'-CCAGACTTCTGCATGGCACGGG-3'